LAWRENCE
LIVERMORE
NATIONAL
LABORATORY

UCRL-TR-213915-REV-1

Microbial Effects on NuclearWaste Packaging Materials

Joanne Horn, Sue Martin, Celena Carillo, Tiangan Lian

September 16, 2005

This work was performed under the auspices of the U.S. Department of Energy by University of California, Lawrence Livermore National Laboratory under Contract W-7405-Eng-48.

Contents

1. Introduction

Microorganisms may enhance corrosion of components of planned engineered barriers within the proposed nuclear waste repository at Yucca Mountain (YM). Corrosion could occur either directly, through processes collectively known as Microbiologically Influenced Corrosion (MIC), or indirectly, by adversely affecting the composition of water or brines that come into direct contact with engineered barrier surfaces. Microorganisms of potential concern (bacteria, archea, and fungi) include both those indigenous to Yucca Mountain and those that infiltrate during repository construction and after waste emplacement.

Specific aims of the experimental program to evaluate the potential of microorganisms to affect damage to engineered barrier materials include the following:

Indirect Effects

- Determine the limiting factors to microbial growth and activity presently in the YM environment.
- Assess these limiting factors to aid in determining the conditions and time during repository evolution when MIC might become operant.
- Evaluate present bacterial densities, the composition of the YM microbial community, and determining bacterial densities if limiting factors are overcome. During a major portion of the regulatory period, environmental conditions that are presently extant become reestablished. Therefore, these studies ascertain whether biomass is sufficient to cause MIC during this period and provide a baseline for determining the types of bacterial activities that may be expected.
- Assess biogenic environmental effects, including pH, alterations to nitrate concentration in groundwater, the generation of organic acids, and metal dissolution. These factors have been shown to be those most relevant to corrosion of engineered barriers.

Direct Effects

- Characterize and quantify microbiological effects on candidate containment materials. These studies were carried out in a number of different approaches, using whole YM microbiological communities, a subset of YM bacteria, and select reference organisms. Studies were carried out to determine morphological alterations to materials surfaces and using electrochemical methods to help quantify effects and modes of MIC, and to provide additional alternative means of evaluating MIC effects. They were carried out only under conservative conditions (low temperature, saturated conditions); thus, resulting conclusions may be considered an upper bound of potential biological effects on tested materials.

2. Present YM Microbial Community and Limiting Factors to Growth

In early studies, organisms were isolated from YM rock by plating on low-nutrient medium. This work was reviewed in the *Engineered Materials Characterization Report for the Yucca Mountain Site Characterization Project,* vol. 3, rev. 1, April 1997, section 2.6 (Reference 1). Microorganisms were isolated at 22° C, 30° C and 50° C under both aerobic and anaerobic conditions. Due to the limited conditions under which organisms were isolated, on growth medium containing an organic carbon source, only heterotrophic organisms (those that require reduced organic compounds as a source of cellular carbon and energy) were obtained. These were subsequently subjected to a battery of tests to determine if any possessed activities associated with corrosion (such as acid production, extrapolymeric or slime production, or sulfide generation through the process of desulfurylation. It was found that many of the isolates obtained had at least one of these activities, thereby showing the potential for MIC at YM. Iron-oxidizing bacteria, which obtain energy from the oxidation of ferrous iron or reduced sulfur compounds and cellular carbon from fixation of carbon dioxide, were also isolated from YM rock on a different medium selective for their growth. The presence of iron oxidizers may be significant for corrosion of carbon steel and titanium as they are capable of denitrification in the absence of an organic carbon source (see Section 4.2.3). Preliminary growth testing of the full complement of microbes contained in YM rock showed insignificant effects of temperature on growth rates or final yields (ca. 10^8 cells/mL added medium) of YM organisms at temperatures up to 50°C in low-nutrient medium. While temperatures above 50°C were not tested in this particular experiment, the results did show some heat resistance of at least a portion of the native YM community.

Later testing, using methods that avoid the need to grow organisms and simply rely on direct extraction of cellular membrane components from rock, showed the cellular density of organisms in YM rock to be approximately $4–7 \times 10^4$ cells/g of dry tuff. A series of experiments to assess growth-limiting factors demonstrated that sufficient nitrate and sulfate were contained in YM groundwater to support microbial growth. However, water availability was judged to be the primary limiting factor to growth. When unamended simulated groundwater was supplied to crushed YM tuff, the cell densities increased by 2–3 orders of magnitude. Secondary limiting factors were found to be both phosphate and organic carbon; when either of these was added to simulated groundwater, cell densities increased 1–2 orders of magnitude. In the absence of added organic carbon or phosphate, heterotrophic cell growth from YM tuff reached ca. 10^6 cells/mL added water. The phosphate required for cellular growth was probably solubilized by microbial acid production directly from YM rock; this process is recognized as commonly occurring and later analysis (presented later in this report) showed this to be the case. Only heterotrophic organisms were counted due to the methods used however, and it is not currently known what these organisms used as a source of carbon while growing in YM groundwater. These results are significant in that after about 1000 years following waste emplacement, groundwater is expected to drip into the repository environment. These experiments showed that significant microbial growth is possible when groundwater becomes available even absent of any added organic carbon (2).

The different types of microorganisms isolated from a given environment by growing on selective growth substrates is necessarily limited; it is estimated that only

0.1–1.0% of the individual species residing in a given sample can be isolated using this approach. Therefore, alternative methods that do not rely on growth were implemented to identify all the members of the extant YM microbial community. DNA was extracted directly from aseptically collected rock, a hyper-variable gene (16S rRNA) that enables species identification was amplified, the resulting clones (200) screened for unique gene sequences, and the results compiled. Sixty-five different species of eubacteria were identified using this approach. The frequency at which individual clonal variants were identified during the screening process allowed some estimation of the relative representation within the total community of each type of organism identified. Metabolic properties of identified organisms, with respect to their potential effects on repository materials, are summarized in Table 1. This work is detailed in Reference 3.

When ventilation was shut off to regions of the Exploratory Studies Facility (ESF), moisture accumulated in unventilated regions and prolific fungal growth ensued. Fungi, which are obligate heterotrophs (i.e., they require a reduced organic carbon source), were found to grow on virtually all organic materials introduced into the ESF. A wide range of species was identified, and air sampling followed by quantification of airborne spores showed over 10^4 fungal spores/m^3 of sampled air in affected areas (in comparison, less than 100 spores/m^3 is found in air outside the ESF). These studies are reviewed in Reference 4. The relevance of fungal growth to integrity of the EBS lies in the capacity of fungi to produce organic acids (e.g., oxalic acid), which may enhance corrosion of Alloy 22. However, these types of organisms require an organic carbon source to grow. Thus, if introduced organic materials are limited in repository construction and design, it seems most likely their growth will likewise be minimal.

Table 1. Potential Effects of Identified YM Microorganisms on Repository Performance

Type of Organisms	Relevant Properties	Potential Effect on Repository
Bacillus, *Clostridium*, *Arthrobacter*	Heat- and desiccation-resistant	May be able to survive initial heat pulse
Caulobacter, *Rhodobacter*	Able to maintain activity at extremely low nutrient levels	Metabolic products produced during low nutrient periods
Pseudomonas, *Arthrobacter*	Able to degrade complex organic compounds	Could degrade plasticizers, plastics, fuels
Microbacterium	Fermentative; produce organic acids and alcohols	Metabolic products can be corrosive to Ni-based alloys
Bacillus, *Pseudomonas*, *Clostridium*	Extracellular products: polysaccharides, enzymes, siderophores, hydrogen	Corrosive; may prevent reoxidation; chelators; potential embrittlement
Many identified organisms	Reduce nitrogen	Alters the chloride/nitrate ratio

3. Microbial Communities under Simulated Repository Conditions

Long-term corrosion testing conditions were evaluated to assess the potential structure of microbial communities under more representative repository conditions. Corrosion tests in the Long Term Corrosion Test Facility (LTCTF), aimed at evaluating candidate engineered barrier materials after long-term exposure under anticipated extreme repository conditions, were analyzed for microbiological colonization. Test vessels are on the order of 1000 L and contain simulated groundwaters at varying ionic strength, pH, and temperature (60°C or 90°C) and material coupons. Deionized water was used as a solvent for dissolved salts. Microorganisms were never intentionally introduced into these systems (no YM rock was included in these tests either); however, they are somewhat open to the surrounding laboratory, and therefore could be inoculated with organisms from the laboratory environment. Initial testing, performed by filtering tank waters with subsequent staining to microscopically visualize organisms, showed the presence of organisms in some tanks. Therefore, further analysis was undertaken to better evaluate the composition of the tank microbial communities, with the expectation that colonizing organisms may be indicative of what organisms would be anticipated to colonize the repository during periods where the environment approached those represented in the LTCTF tanks.

The composition of microbial communities in three LTCTF tanks was determined using direct DNA extraction of tank waters and swipes. Several liters of water were filtered from each sampled tank, and filters were combined with swabs that had been used to swipe the inner tank walls. Filters and swabs were pooled; and adsorbed organisms were desorbed and subjected to DNA extraction, 16S rDNA amplification, and cloning of amplified regions (as above). One hundred clones were screened from each tank to identify unique sequences/organisms and the clonal frequency of each unique sequence was calculated, based on the 100 clones screened (Fig. 1). Water and swipes were also assessed by phospholipid fatty acid (PLFA) analysis, which provides an estimate of total bacterial density (data not shown), and direct microscopic counts to provide another means of determining bacterial densities (Table 2).

As deduced from the bacterial density assessments (Table 2), bacteria were detected under all conditions tested. However, the greatest concentrations were associated with a 10-fold increased ionic strength of groundwater at 60°C, while the lowest densities were found in acidified, concentrated (1000×) groundwater. In terms of the types of organisms that colonized in the 60°C tanks tested, generally it was found that each tank contained a different community of organisms. This finding shows that in selective environments, those organisms best adapted to a particular set of conditions will prevail.

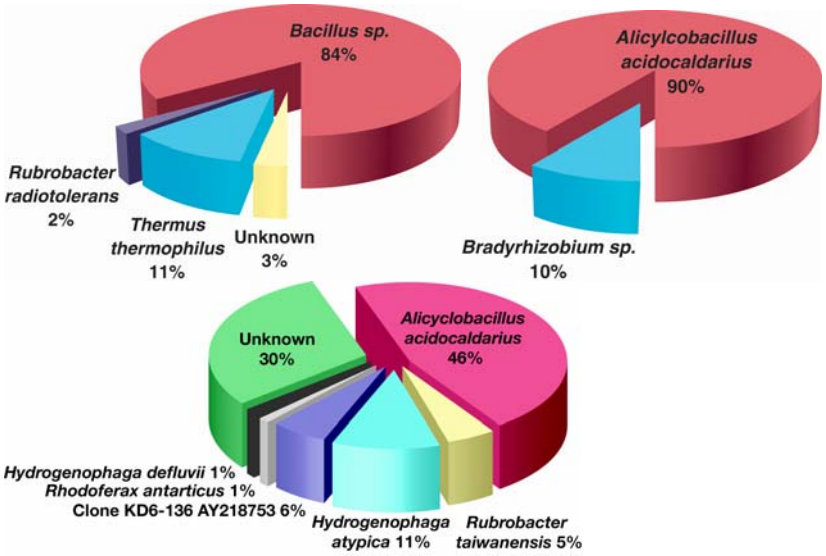

Fig. 1. Frequency of unique clone types (whose sequences indicate species) in LTCTF tanks. After amplification and cloning of 16S rRNA genes, 100 clones were screened; the frequency of occurrence of unique clones is depicted as the percentage of the total number of clones screened.

Table 2. Cell Density of LTCTF Samples Determined by Direct Microscopic Counts

LTCTF Sample	Direct Microscopic Counts* (cells/mL)
1000× groundwater, pH 2.8, 60°C	1.30E+04
1000× groundwater, pH 10.3, 60°C	1.19E+05
1000× groundwater, pH 10.3, 90°C	1.31E+06
10× groundwater, pH 10.1, 60°C	4.60E+06
10× groundwater, pH 10.1, 90°C	4.87E+05

*Desorbed cells from these samples were stained with Acridine Orange before microscopic counting in a chamber of known volume.

Alicyclobacillus acidocaldarius, which was a major component of the concentrated groundwater communities at both pH 2.8 and 10.3, has otherwise been isolated from acidic hot springs and contains hopanoid membrane lipids that harden the membrane to caustic or highly concentrated solutions. Although none of the identified organisms (with the exception of *Bacillus*) is generally known to inhabit environments such as those typified by the LLNL laboratory or Livermore, CA, in general, they were apparently able to transport to and colonize the LTCTF tanks. This demonstrates the broad distribution of organisms normally thought to inhabit extreme environments (such as hot springs) and supports the general tenet that transport is not a limiting factor for microbial colonization; it is generally thought that the environment is the selective force that determines which organisms inhabit a specific locale. Organisms that are able to survive in a given environment and are best suited to exploit the resources available. The organisms that colonized these tanks, therefore, may be an indicator of those that may colonize the repository environment during periods when conditions are similar to those in the LTCTF tests.

4. Microbiological Effects on Water Chemistry

4.1. Acid Generation and Associated Decrease in pH

The production of organic acids as products of microbial central metabolism is well documented (e.g., Reference 15, particularly Chapter 9; Reference 16, “Part II: Bioenergy and Metabolism”). The generation of acids has been both directly and indirectly linked to metal corrosion. Microbially generated acids have been shown to directly dissolve the protective calcareous film on stainless steel. Coupling of protons with electrons results in electron removal from the cathode, and forms hydrogen, which is a substrate for microbial sulfate reduction. Therefore, individual strains isolated from YM rock were screened and tested under various conditions for their effects on pH of the bulk growth medium. Results revealed that both growth and acid production were generally more rapid when the media were amended with glucose. This is not surprising given that acid production is largely a result of organic carbon utilization; addition of glucose provides at once more carbon and energy for growth, together with a greater potential rate of acid generation. However, about 10% of YM strains tested showed decreases in medium pH even without carbon addition. The lowest pH attained was 4.2. These results are further discussed in Reference 1.

Further experiments were carried out using the entire complement of organisms contained in YM rock, under varying growth conditions. It was found that sodium carbonate-based groundwaters (which are predicted to represent the bulk of repository seepage waters) effectively buffered biogenic acid production resulting in the maintenance of near neutral pH in the bulk solution. These findings are further detailed in Reference 5.

Fungal growth from YM rock was also tested for its effects on pH under a variety of conditions. When media containing adequate nutrients specific for fungal growth (i.e., high concentrations of reduced organic carbon) were employed, the pH of the medium was reduced to pH 3. However, when YM fungi were grown from YM rock in a simulated YM ground, water increased in ionic strength tenfold (from that found in situ,

10× J13). Initially, the pH decreased to pH 5 but was subsequently found to increase somewhat to pH 6, demonstrating the possible buffering effects of the sodium carbonate-based groundwater.

Sodium carbonate-based seepage waters have thus been shown to buffer the effects of potential acid production by microorganisms within the repository. This may counter the corrosive effects of microbial and fungal generated acids. However, it may also be important to consider that the measurements of pH effects have only been conducted on the bulk aqueous phase in which these organisms are growing. Within biofilms, the accumulation of cells and extracellular products produced by these organisms on surfaces, the concentrations of acids may be much greater than those that have been diluted in the surrounding medium. Furthermore, it is not known how well this observed buffering effect would function within the semi-solid biofilm matrix.

The types of organic acids generated by bacteria and fungi that have been found to accumulate on rock substrates include low concentrations (nM–µM) of lactate, formate, and oxalate. These same organisms grown under simulated in situ conditions have been shown to produce µM–mM concentrations of a broader range of organic acids including succinate, citrate, malate, pyruvate, and fumarate (6). Pure fungal cultures of *Aspergillus*, a fungi found to be prevalent in the ESF, has been shown to produce oxalate at a rate of 1.5 mM/hr (7); however, fungi do require a reduced carbon source to generate acids, and presumably, these would be minimal in the planned repository. Scoping studies were conducted with the full complement of organisms contained in YM rock with a continual feed of simulated concentrated groundwater (10× J13 with 0.1% glucose). Results of these studies show a steady-state concentration of acetate in the bulk aqueous phase of 3.2 mM and formate at 0.34 mM; lactate was detected (0.22 mM) in bulk cultures of YM rock containing microorganisms incubated with 10× J13 (with glucose). *Thiobacillus*, an iron- and sulfur-oxidizing organism that fixes carbon dioxide to supply cellular carbon and found in YM rock samples, generates formate (0.12 mM) in continuously fed cultures grown on a sulfur-based medium. A sulfate-reducing bacterium was found to generate acetate (40 mM) from lactate. Concentrations of these acids, as they were measured in the bulk aqueous phase of the cultures, do not appear great enough to affect corrosion of proposed EBS materials, and oxalate has not been found to affect breakdown of the Alloy 22 passive film in simulated crevice solutions. However, as was pointed out concerning overall pH effects, concentrations of organic acids may be expected to be much greater in biofilms colonizing these materials.

4.2. Nitrate Reduction

Nitrate counters the corrosive effects of chloride ions. The nitrate/chloride ratio of evolved groundwaters in the proposed nuclear waste repository at Yucca Mountain has therefore been acknowledged to be an important aspect to factor into the overall evaluation of potential corrosion of repository engineered barriers. Nitrate/chloride ratios above 0.2 to 0.5 have been shown to inhibit Alloy 22 corrosion, the proposed waste package corrosion barrier. Both nitrate and chloride are components of YM groundwater, present for example in J13 well water at concentrations of 0.155 mM and 0.195 mM, respectively. Microbiological reduction of nitrate may occur, causing a decrease in the nitrate/chloride ratio, thereby potentially contributing to corrosion of barrier materials.

4.2.1. Modes of Nitrate Reduction

Bacteria can reduce nitrogen by a number of different modes (Fig. 2). Nitrate can be directly incorporated into cells, then reduced intracellularly and incorporated into proteins, nucleic acids, and other cellular components (i.e., assimilated via anabolic metabolism). Assimilation of nitrate has been shown, however, to comprise a very minor component of overall nitrate consumption in soils and is relatively insignificant when compared to dissimilatory processes. This is because many nonphotosynthetic microorganisms are unable to reduce oxidized nitrogenous compounds for assimilation, so they must be supplied in a reduced state.

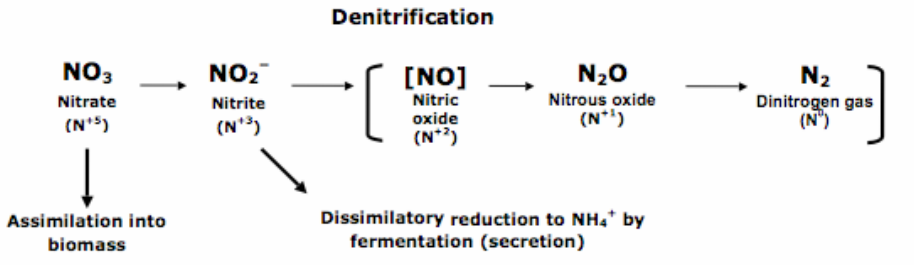

Fig. 2. Microbiological pathways of nitrate reduction. Names of specific compounds are designated together with the oxidation state of nitrogen in parentheses. The role of nitric oxide has been debated.

Alternatively, in microorganisms capable of carrying out fermentation (whereby a reduced organic substrate acts as both an electron donor and acceptor; one component of the original organic substrate is oxidized and the other reduced), a process known as dissimilatory nitrate reduction to ammonium (DNRA) results in the production of secreted ammonium from nitrate. This process has been determined to be favored when elevated organic carbon/nitrate ratios are prevalent. High nitrate concentrations are also required for DNRA to occur because generally the enzymes involved in the process have a low affinity for nitrate (100–500 µM). Greater redox potentials in addition to the requirement for elevated organic carbon also favor DNRA. The requirement for greater concentrations of fermentable organic carbon than of nitrate for DNRA to proceed makes it unlikely that this process will occur to any significant extent in the projected repository environment, as long as available carbon sources remain minimal.

4.2.2. Heterotrophic Denitrification

DNRA is distinguished from what may be termed “true” denitrification, which refers to the use of nitrate as a terminal electron acceptor with the evolution of nitrogenous gaseous products (as indicated in Fig. 2). Many aerobic organisms that use organic carbon as a source of energy and carbon (i.e., “heterotrophs”) and normally employ oxygen as a terminal electron acceptor are capable of using nitrate in this latter

capacity if it is available in sufficient concentration. The process of heterotrophic denitrification can be represented by the following chemical reaction, using glucose as a model organic compound/electron donor:

$$4NO_3^- + 5/6\ C_6H_{12}O_6 + 4H^+ \rightarrow 2N_2 + 5CO_2 + 7H_2O$$

It has been estimated that denitrifying organisms comprise 1–5% of the total heterotrophic microbial community and 20% of the total anaerobic community (i.e., those organisms capable of using terminal electron acceptors other than oxygen) in soils. The bulk of these denitrifying organisms are adsorbed to particulate soil and mineral surfaces. In terms of the taxonomic distribution of microorganisms that carry out denitrification, *Alcaligenes*, *Bacillus*, *Corynebacterium*, and *Pseudomonas* isolates all have denitrification capacity; *Pseudomonas* and *Alcaligenes* have been implicated as major contributors to denitrification worldwide. All of these types of organisms have been identified as members of the microbial community now extant at Yucca Mountain. However, in addition to the ability to carry out denitrification, three other general requirements are necessary for denitrification to occur:

- Presence of nitrogen oxides
- Suitable electron donors
- Restricted oxygen availability

Clearly, nitrate is present in YM groundwaters presently; therefore, denitrification is not occurring to any major extent now. Restricted oxygen availability is not necessarily a relevant limiting factor because it is generally acknowledged that anaerobic microsites regularly occur in geologic media. Therefore, presence of suitable electron donors is the primary factor that may well limit the extent of denitrification now and whether denitrification will occur during repository evolution.

4.2.3. Autotrophic Denitrification

Some bacteria are capable of using nitrogen as a terminal electron acceptor (in place of oxygen) using inorganic, rather than organic electron donors. These organisms use either reduced sulfur compounds or ferrous iron as electron sources and are able to fix carbon dioxide to supply cellular carbon, so-called “autotrophic” metabolism. Thus, these types of organisms do not require an organic carbon source; they derive both their energy (electron) and carbon sources from inorganic compounds. It had been observed that ferrous iron–containing groundwaters never contained nitrate. This was originally thought to be a result of the abiotic chemical reduction of nitrate by Fe^{+2}, which had been observed in the presence of Cu^{+2} catalysts at circumneutral pH. However, attempts to observe denitrification in Fe^{+2}-containing aquifer samples that had been sterilized failed. Shortly thereafter, it was reported that *Gallionella ferruginea*, an autotrophic organism deriving reducing equivalents from ferrous iron, is able to reduce nitrate to nitrite. Nitrate can then be reduced to gaseous nitrogenous products by the oxidation of Fe^{+2} to Fe^{+3} via reactions including:

$$HNO_2 + Fe^{+2} + H^+ \rightarrow NO + Fe^{+3} + H_2O$$

$$2NO + 2Fe^{+2} + 2H^{+} \rightarrow N_2O + 2Fe^{+3} + H_2O$$

$$2HNO_2 + 6Fe^{+2} + 6H^{+} \rightarrow N_2 + 6Fe^{+3} + 4H_2O$$

Another autotrophic organism, *Thiobacillus denitrificans*, which oxidizes reduced sulfur (sulfide, thiosulfate, or elemental sulfur) to sulfate as an electron source, can use nitrate as a terminal electron acceptor. A series of field studies found that this organism caused the reduction of nitrate to nitrogen gas at the expense of endogenous ferrous disulfide (or pyrite):

$$5FeS_2 + 14NO_3^{-} + 4H^{+} \rightarrow 7N_2 + 10SO_4^{-2} + 5Fe^{+2} + 2H_2O$$

There is evidence that the ferrous iron produced as a product in this reaction also acted in an autotrophic biotically mediated process to reduce nitrate. Well waters containing ferrous iron were amended with nitrate and incubated; subsequent analysis showed decreases in nitrate and increases in ferric iron according to the following stoichiometry:

$$5Fe^{+2} + NO_3^{-} + 7H_2O \rightarrow 5FeOOH + 0.5N_2 + 9H^{+}$$

A study examined the geochemistry of a nitrate-containing aquifer that contained both pyrite and deposits of organic matter in the form of brown coal. The conclusion was that the bulk of denitrification, which was found in a region where the redox potential dropped sharply, was mainly fueled by pyrite as the principal electron donor; only 15% of nitrate reduction used the coal as an electron donor. However, this same report showed that although sulfate concentrations increased in the nitrate-reducing zone, ferrous iron remained, indicating that the Fe^{+2} generated by incomplete pyrite oxidation did not further contribute significantly to nitrate reduction.

Autotrophic denitrification has not been as extensively studied as heterotrophic denitrification; therefore, it is presently not clear how widespread or common this process is in various environments. Almost all studies to date regarding biogenic denitrification have focused on heterotrophic processes; the limiting factors and kinetics of the autotrophic physiology and metabolism are largely unknown. However, it has been shown in many field and laboratory studies that bacterial denitrification overall is often organic carbon-limited, indicating that autotrophic denitrification may not play a significant role in situ in reducing nitrates. However, if autotrophic denitrification were a factor in the evolution of the YM repository, it would decouple the requirement for organic carbon to fuel denitrification; denitrification could proceed without the need for organic carbon, fueled only by groundwater carbonate, and reduced iron or reduced sulfur.

4.2.4. Field Rates of Denitrification

Measured rates of denitrification in the unsaturated zone are more relevant to the anticipated conditions in the YM repository, since the repository horizon will be perched approximately 300 meters above the water table. However, very few studies have been conducted examining vadose zones at depth (>10 meters) in the subsurface. Both a study assessing denitrification activity to 289 meters in sand and clay and one determining

denitrification in limestone and overlying units to 180-meter depth did show significant decreases in denitrification with sampling depth (8, 9). The latter study showed a 100-fold lower denitrification rate (1.7 nM NO_3/g/day) at depths of 40 meters or greater than in surface soils. Deep clay sediments demonstrated little or no activity, which may be due to the lack of permeability in clays to infiltrating nitrate; in fact, this same study did show the *potential* for denitrification at all depths examined if nitrate were added to withdrawn sediment samples. Measurements in a sand/clay study below 150 meters deep in unamended samples show denitrification rates on the same order as those seen in limestone if no nitrate is added. Yet, if nitrate became available, rates increased up to 100-fold, demonstrating that denitrifying organisms were present in the deep sediments but required appropriate conditions to be active (8).

4.2.5. Observed Conditions for Nitrate Depletion of YM Groundwater

As noted above, organisms capable of carrying out at least heterotrophic denitrification are currently present within YM rock. Therefore, it could be that the limiting factor to denitrification presently in the YM subsurface is a lack of organic carbon or inorganic electron donors. It is unlikely that sufficiently reducing conditions are a limiting factor because anaerobic microsites are assumed to be available in geologic media. Recent experimental evidence, though, shows a somewhat more complex picture. Complete or near complete elimination of nitrate by YM organisms contained in YM rock supplied with a constant feed of simulated 10× J13 amended with 0.1% glucose was observed when either Alloy 22 or Stainless Steel 316 (SS 316) was present. Identical systems (Fig. 3) containing sterilized rock maintained the same approximate concentration of sulfate found in the background 10× J13 + 0.1% glucose (Table 3 and Fig. 4). Therefore, in the presence of these two alloys, either denitrification or nitrate assimilation was occurring. However, in systems run under the same conditions but

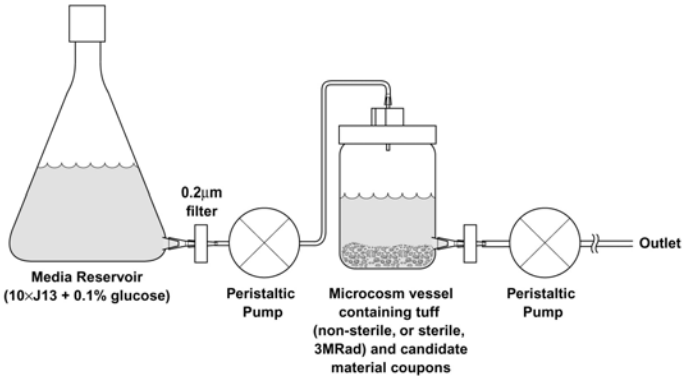

Fig. 3. Overall configuration of continual flow microcosms simulating a saturated repository environment. Simulated concentrated sodium carbonate-based groundwater amended with glucose was fed (2 mL/h) into a vessel containing either sterile or non-sterile YM rock and candidate material coupons. Microcosms were incubated at room temperature (22°C) or 30°C. Effluent was sampled on the outlet for chemical analysis. Periodically, coupons were withdrawn for surface analysis.

Table 3. Nitrate Depletion* in Saturated Repository Microcosms

EBS Material	Presence of YM Organisms	
	Unsterilized Rock	Sterilized Rock
Alloy 22	+	–
Stainless Steel 316	+	–
Titanium grade 7	–	–
No alloy	–	–

*Observed nitrate depletion is indicated by (+); lack of nitrate depletion is indicated by (–).

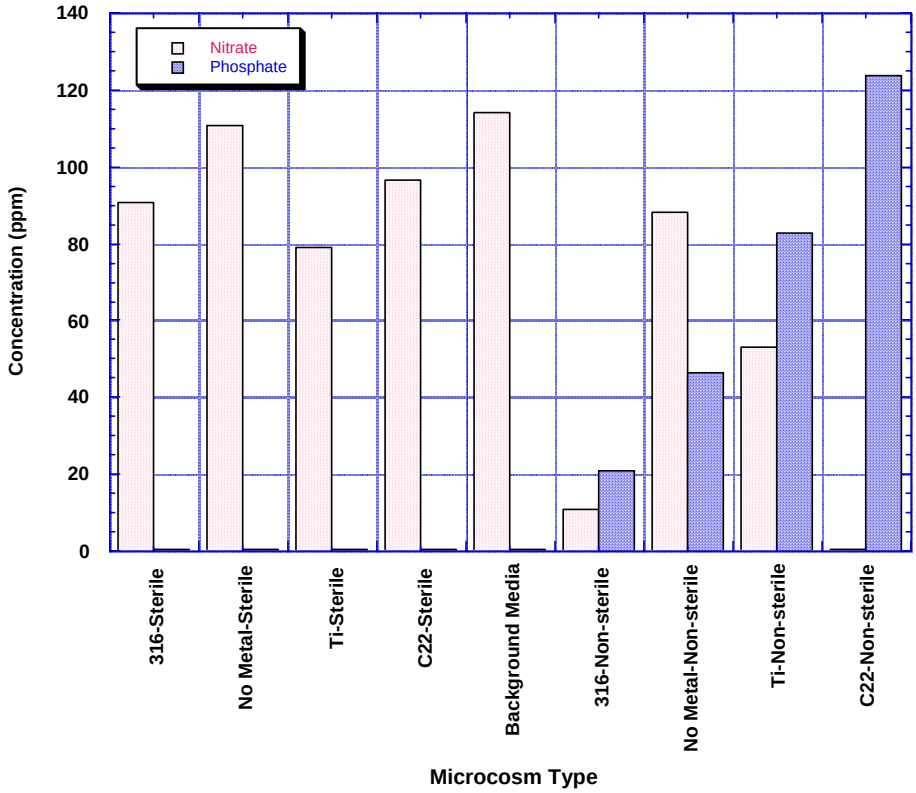

Fig. 4. Phosphate and nitrate concentrations in microcosm efflux solutions (i.e., spent 10× J13 + 0.1% glucose) from microcosms containing either different candidate EBS materials or no EBS materials. Concentrations of anions were determined using ion chromatography.

containing either no metal alloys or titanium grade 7 (Ti gr7), no significant reduction (no metals) or little reduction (Ti gr7) in nitrate concentration was observed in the presence or absence of YM microorganisms. (cf. Table 3 and Fig. 4).

The lack of nitrate depletion in microcosms containing either no metals or Ti gr7 strongly suggests that nitrate assimilation was not occurring in the vessels containing Alloy 22 or SS 316, because it would be generally expected for nitrate assimilation to occur equivalently under all tested conditions, no matter the type of alloy (or lack thereof) present. Likewise, if the glucose contained in the feed water were the source of reducing equivalents for nitrate reduction, then it would be expected for nitrate reduction to occur similarly across the types of alloys, since glucose was present in all microcosms. However, if autotrophic denitrification were occurring with an alloying component of Alloy 22 and SS 316 serving as an electron donor (while Ti gr7 could not supply reducing equivalents as readily) for nitrate reduction, then one might expect the observed result. An alternative explanation could be that microcosms containing different alloys contained different microbial populations because conditions encouraged the growth of differential populations of microbes from the rock, of which some were capable of nitrate assimilation or reduction, while others were not.

5. Materials Testing

5.1. Micrometer-Scale MIC of Alloy 22 in Saturated Repository Microcosms

5.1.1. Coupon Surface Analysis

Coupons of Alloy 22 were exposed to a simulated, saturated repository environment consisting of crushed rock from the repository site and a continual flow of simulated groundwater supplemented with 0.1% glucose (as was depicted in Fig. 3) for periods up to five years. Coupons were incubated with YM tuff that was either left unsterilized (with the YM microbial community left intact) or was pre-sterilized prior to being placed in the experimental vessels; vessels were incubated at either room temperature or 30°C. Surface analysis of the biotically incubated coupons shows development of both submicrometer sized pinholes or micropores; these features were not present on either sterile or untreated control coupons. The micropores formed on the Alloy 22 coupons exposed to be biotic environments are also referred to as micropits or micropitting in this document.

Alloy 22 coupons from microcosms incubated at 30°C were withdrawn, cleaned, and imaged using scanning electron microscopy (SEM). An unreacted Alloy 22 coupon was also cleaned and imaged in parallel for comparison. These SEM results are shown in Fig. 5. Coupons incubated in the non-sterile microcosm reactors showed the development of pinholes, primarily along the ridges formed by polishing, while coupons incubated in sterile microcosms and those that were not reacted in microcosms showed no evidence of pinhole formation after one cleaning cycle. The micropits appeared uniform in shape except where they had grown together and ranged in size from 200–700 nm in diameter.

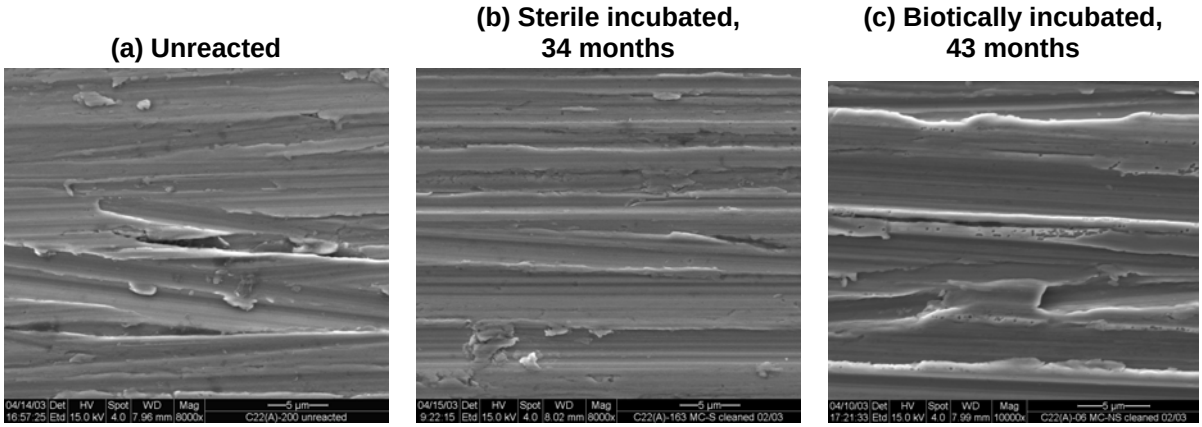

Fig. 5. Alloy 22 coupons incubated at 30°C: (a) unincubated/nonreacted coupon; (b) sterile-incubated coupon, and (c) non-sterile-incubated coupon. Coupons were cleaned and interrogated using scanning electron microscopy at a magnification of 8000× (a and b) or 10,000× (c). Pinhole formation, along the ridges formed by polishing, was evident on non-sterile coupons incubated 43 months (c), while sterile coupons incubated 34 months (b) and unreacted coupons (a) did not display pinhole formation.

In contrast to the Alloy 22 non-sterile coupons incubated at 30°C, coupons withdrawn after long-term incubation from biotic microcosms incubated at 22°C showed markedly different patterns of micropitting. Again, small micropores (generally less than 1 μm) were apparent on the surface, but their distribution and frequency was extensive, covering all regions of the coupon, and not restricted to polishing ridges. Furthermore, the micropores were less uniform in shape and size compared with those observed on the 30°C incubated coupons (Fig. 6). Coupons analyzed prior to cleaning contained a micropore density similar to those that were cleaned; cleaning effects, if any, were not observed. Unreacted coupons and those incubated under sterile conditions did not show micropore formation (Fig. 6). Coupons incubated biotically at room temperature for shorter durations (17 months and 32 months) also demonstrated micropore formation, indicating that the micropores were generated at the earlier sampling time points. Gravimetric analysis was inconclusive because many of the micropores were filled with deposited or precipitated minerals. Energy dispersive spectral analysis of pitted coupons showed that the micropits were often filled with siliceous material, which apparently originated from either dissolved and re-precipitated silica or particulate fines from the YM rock. Aluminosilicates were also present.

Atomic force microscopy (RMS analysis) indicated that the overall roughness of the non-sterile coupon surfaces incubated at ambient temperature decreased as a function of time, indicating a flattening of the coupon surface, even as microscale roughness increased due to micropore formation. Micrographs (SEM) also demonstrate surface smoothing; the polishing ridges have flattened, and only the gross features, such as surface gouges, remain (Fig. 6). The distribution of surface roughness (which includes the effect of micropores on biotically incubated samples) was evaluated using imaging analysis (Image Tool, v. 3.00, University of Texas Health Science Center, San Antonio; http://ddsx.uthscsa.edu/dig/itdesc.html) of SEM micrographs of Alloy 22 coupons incubated in microcosms for six years at ambient temperature. For sterilely incubated

coupons (3 coupons examined, a total of 15 fields analyzed), the median roughness density was 8.39 $\mu m^2/mm^2$ of coupon surface (maximum value 18.60 $\mu m^2/mm^2$; minimum value 0.021 $\mu m^2/mm^2$). For a biotically incubated coupon (10 fields analyzed), the median roughness density was 17.83 $\mu m^2/mm^2$ (maximum value 27.78 $\mu m^2/mm^2$; minimum value 9.45 $\mu m^2/mm^2$). Thus, the roughness density of biotically incubated samples is higher than that for sterilely incubated samples by a factor of about two (in large part due to the development of micropores). Because the depth associated with the difference in roughness could not be determined, the difference in total metal loss could not be estimated from the imaging analysis.

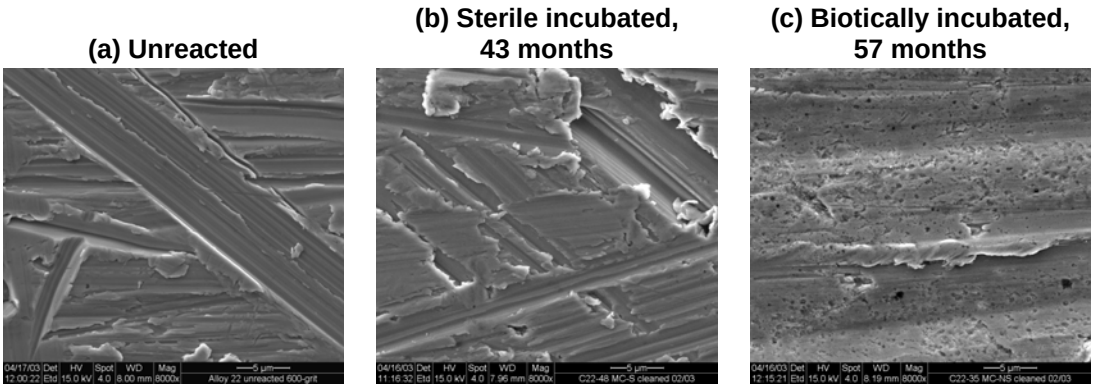

Fig. 6. Alloy 22 coupons incubated at room temperature (22° C): (a) unincubated, nonreacted coupon; (b) sterile incubated coupon (43 months); and (c) non-sterile incubated coupon (57 months). The micropores on the non-sterile coupons were ubiquitous and not uniform in shape (c).The unreacted (a) and sterile (b) surfaces are similar in appearance and are free of micropore features. All images are magnification 8000×.

It is not entirely clear why the distribution and frequency of micropores differ between biotically incubated coupons at room temperature as opposed to at 30°C. Clearly, the environments differ enough to create a sharply contrasting pattern of micropitting. This may be due to differences in the microbial communities, a result of the proliferation of different organisms from a single community when they are incubated under varying conditions (here, a temperature difference). To further probe this possibility, we performed analysis of the microbial communities, those pelagic organisms in the solution phase, and those adhered to coupons, in biotic room-temperature and 30°C microcosms. Purification of single colonies (which represent growth from a single cell) from microcosms incubated at room temperature and 30°C was undertaken, and these were identified using 16S rDNA analysis. The results showed that there were completely different microbial communities present in microcosms incubated at different temperatures, at least in terms of those that were culturable on the medium used for isolation (R2A, a low-nutrient formulation). In the room-temperature microcosm sampled, a *Pseudomonas* sp. and *Burkholderia cepacia* were identified, while the 30°C-incubated microcosm had an unrelated culturable community structure that included *Ralstonia pickettii*, *Sphigomonas paucimoblis*, and *Bacillus licheniformis*. The varying activities of these organisms may well account for the observed differential effects on Alloy 22 under these two test conditions.

5.1.2. Dissolution of Alloy 22 Determined by Effluent Chemical Analysis

Chemical analysis of bulk aqueous efflux solutions from microcosms were undertaken to determine the concentration of solubilized Alloy 22 elements. Solubilized metal from the coupons and contributions from the tuff and growth media were identified with ICP-MS on samples from sterile and non-sterile microcosms incubated at 30°C or room temperature. Note that ion chromatographic analysis of these same fluids resulted in the observations shown previously in Fig. 4.

A seven- to sixteen-fold elevation in Mn concentration was detected in the 30°C-incubated, non-sterile microcosm reactors containing tuff and metal coupons (exceeding 600 ppb), compared to the background media, the no-metal, non-sterile control reactors containing tuff (86 ppb), and sterile control reactors containing coupons and tuff (38 ppb) (Fig. 7a). Manganese is a component of both Alloy 22 and YM tuff; therefore, the Mn concentration in the no-added-metal, non-sterile reactors reflects Mn solubilized solely from tuff in the presence of YM bacteria (Mn concentration in YM tuff is 0.05–0.06 wt % and 0.26 wt % in Alloy 22). Sterile control reactors that contain Alloy 22 coupons and tuff contained small amounts of solubilized Mn in the absence of microbial activity. Since the Mn concentration was 86 ppb in the no-metal, non-sterile control reactors and 38 ppb in the sterile control reactor effluent, it is evident that the majority (>80%) of solubilized Mn in the non-sterile, 30°C reactors arose from the Alloy 22 coupons due to microbial activity. These findings were in contrast to those from the room-temperature-incubated microcosms, where chemical analyses of the bulk aqueous efflux solution did not indicate elevated concentrations of metals and dissolved salts above background and control concentrations, indicating that the metal lost from the surface had been either precipitated or adsorbed.

Molybdenum in 30°C-incubated non-sterile, coupon-containing microcosm reactor effluent was also elevated above background and control values, but the absolute concentration was low (10 ppb). The no-metal, non-sterile control was measured just above detection limits (0.4 ppb; Fig. 7b), showing that very little to none of the Mo originated from tuff. The coordinate sterile control reactors also contained Mo at levels just above detection, indicating that the solubilized Mo in non-sterile reactor effluent may have been due to microbial activity. These experiments are further discussed in Reference 10.

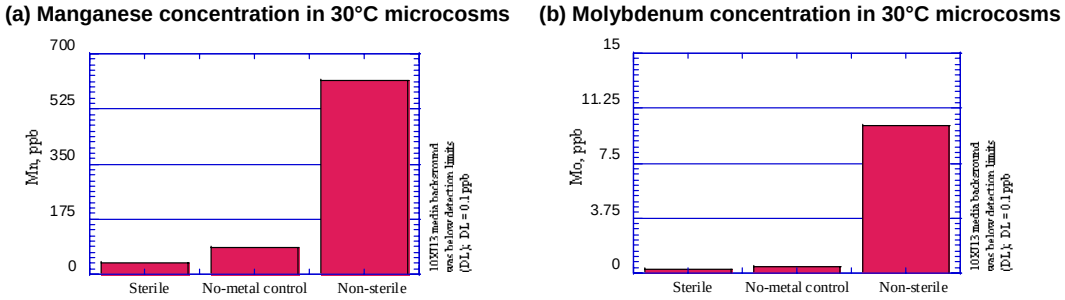

Fig. 7. Chemical analysis of bulk aqueous solutions from microcosm reactors incubated at 30° C shows that (a) there is an increase in soluble Mn compared to the no-added-metal, non-sterile and sterile controls and (b) molybdenum was detected in low concentrations in the non-sterile reactors but at higher values than for the sterile and no-added-metal (non-sterile) controls.

5.2. Biogenic Titanium Dissolution

An experiment was undertaken to evaluate more extreme conditions under which EBS materials might be susceptible to MIC. Iron-oxidizing organisms cultured from YM rock samples use carbon dioxide as a source of cellular carbon and derive energy from the oxidation of reduced sulfur or iron. *T. ferrooxidans*, a sulfur- and iron-oxidizing bacterium, was grown in continuous culture, with a constant supply of a growth medium containing thiosulfate as an energy source, generating sulfuric acid as an end product of metabolism. Culture conditions were aimed at generating an exponential-phase culture in which the organisms were metabolically vigorous over an extended period; material coupons were exposed to this continually growing culture throughout the incubation period of seven months. Our findings show that there was no discernable corrosion of Alloy 22; however, Ti gr7 did show signs of generalized corrosion on a micrometer scale using atomic force microscopy (AFM, Fig. 8). Consistent with signs of Ti gr7 corrosion observed using AFM, deposition of (presumably solubilized) Ti was found in the reactor and on Alloy 22 coupons resident in the same reactor as the Ti coupons (Table 4). Titanium coupons exposed to sterile thiosulfate medium did not display any signs of corrosion, thereby implicating *T. ferrooxidans* metabolic products of thiosulfate as potential corrosive agents on titanium. These results are further delineated in Reference 11.

These experiments show that given the appropriate growth conditions, particularly with respect to supplying a reduced sulfur compound as an energy source, sulfur-oxidizing organisms can enhance some corrosion of Ti gr7. Sources of reduced sulfur in the repository may be limited, however, possibly obviating this corrosion route.

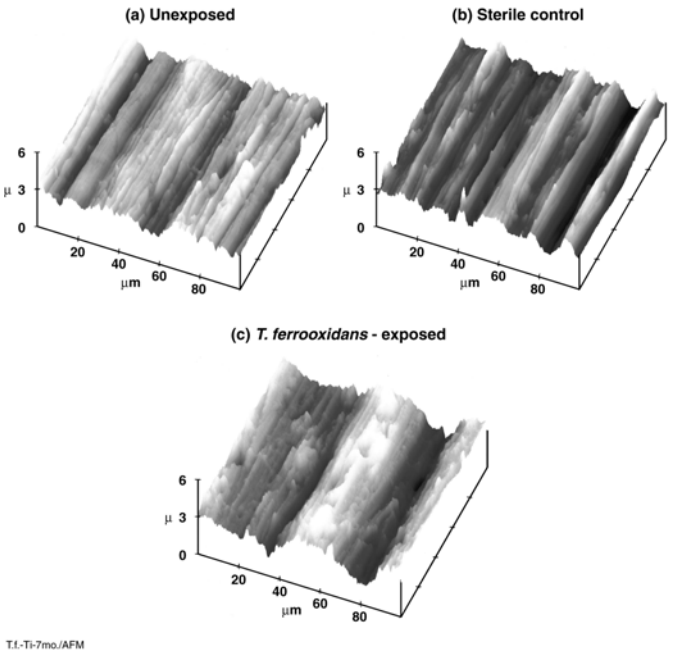

Fig. 8. AFM images of titanium grade 7 after fixation and acid washing: (a) unexposed starting material coupon; (b) after seven months incubation in sterile Thiosulfate medium alone; and (c) after seven months incubation in *T. ferrooxidans* culture grown in Thiosulfate medium.

Table 4. Elemental Analysis of *T. ferrooxidans* Bioreactor Effluent and Precipitates

Sample	Cr (mg/L)	Ni (mg/L)	Ti (mg/L)
Filtered effluent	1.36	0.521	0.023
Unfiltered effluent	0.98	0.352	0.023
Precipitate	0.19	0.068	0.269
Detection limit	0.01	0.01	0.02

5.3. Electrochemical Testing to Assess Corrosion Rates and Modes

Previous electrochemical testing showed relatively low rates of generalized corrosion (using polarization resistance measurements) of Alloy 22 in the presence of YM microorganisms, using unaerated batch systems supplied with a rich nutrient medium. The mean rates of corrosion of Alloy 22 in these systems, with the addition of YM microbes, was 0.2 μm/y. Biotic systems showed a twofold increase in corrosion rate compared with identical systems run under sterile conditions. Under these test conditions, anodic polarization behavior of Alloy 22 base metal shifted toward slightly higher current densities at lower applied potentials when YM bacteria were present versus in their

absence, indicating that YM bacteria caused somewhat greater anodic activity, in agreement with the observed increase in corrosion rates. These results are discussed further in Reference 12.

In a follow-on study, conditions were modified to: (a) provide a more representative aqueous medium, (b) generate a system that would not become nutrient- or oxygen-depleted over the test period, (c) enable better endpoint analysis of coupon surfaces, and (d) incorporate additional types of test materials than had been tested previously. These ends were accomplished by incorporating the following factors into the test plan:

- Simulated 100× J13 supplemented with phosphate and 0.1% glucose was used as a feed medium, to better simulate seepage waters; phosphate was added to mimic bacterial dissolution of phosphate from YM rock (as was depicted in Fig. 4).
- Vessels were fed in a constant flow mode (2 mL/h) with feed medium.
- Vessels were constantly sparged with air.
- Mirror finished coupons were used.
- Alloy 22 base metal, Alloy 22 weldments, and Ti gr7 base metal were tested.
- Tests were conducted under sterile and MIC (YM bacteria) conditions.
- All trials were performed in triplicate.

The test matrix is outlined in Table 5.

Table 5. Testing Matrix For Polarization Resistance Experiments on Alloy 22 and Ti Gr 7.

Specimens	Vessels	
	Sterile	Non-Sterile
Alloy 22 Non-Welded (MA)	7, 8, 9	16, 17, 18
Alloy 22 As-Welded (ASW)	1, 2, 3	10, 11, 12
Ti Gr 7 Non-Welded	4, 5, 6	13, 14, 15

Vessels 1-18 were in operation for several months. The time of operation was different for each vessel. The corrosion potential and the polarization resistance of the specimens exposed to vessels 1-18 were monitored regularly. The polarization resistance is inversely proportional to the corrosion rate. Results show that the corrosion potential (E_{corr}) for welded and non-welded Alloy 22 coupons more or less stabilized for exposure times higher than 125 days. For Ti Gr 7, the E_{corr} stabilized for times higher than 75 days. For the entire testing time, the polarization resistance measurement showed considerable scattering, both for the sterile and non-sterile environments. The corrosion rate (calculated from polarization resistance measurements) for the specimens exposed to both types of environments was averaged for times higher than 125 days (for Alloy 22) and for times higher than 75 days (for Ti Gr 7).

Figure 9 shows the average corrosion rate for welded and non-welded Alloy 22 specimens. The standard deviation is represented as error bars. For both types of Alloy 22

specimens, the corrosion rate in the non-sterile environment was slightly higher than the corrosion rate in the sterile environment by a factor of approximately two.

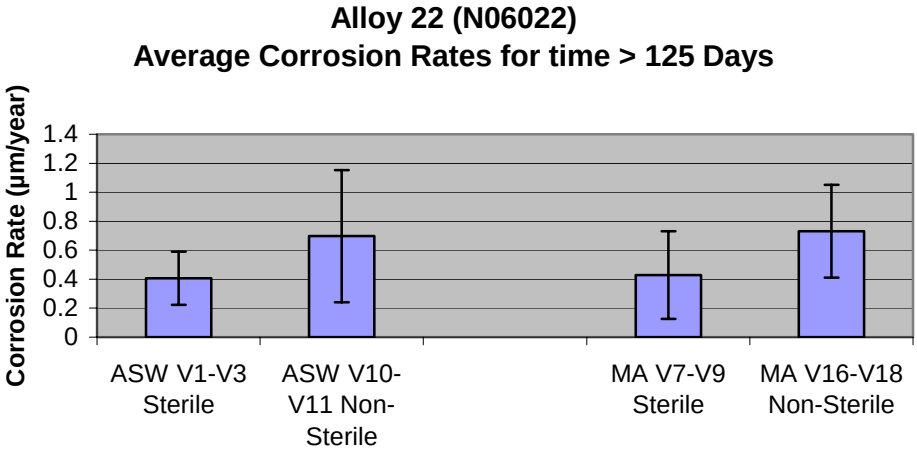

Fig. 9. Average corrosion rates determined by polarization resistance testing of welded and non-welded Alloy 22 for times higher than 125 days.

Figure 10 shows the average corrosion rates for Ti Gr 7 in sterile and non-sterile environments. For the sterile environment, the data from Vessel 5 was not included since it showed high corrosion rates. As was the case for Alloy 22, for Ti Gr 7 the corrosion rate in the non-sterile environment was higher than in the sterile environment approximately by a factor of two. The standard deviation for Ti Gr 7 in non-sterile conditions was larger than for Alloy 22 and considerably overlapped the data for the sterile Ti Gr 7.

Anodic polarization experiments were conducted on welded (Fig. 11) and base metal (Fig. 12) Alloy 22 specimens that had been reacted with and without inoculated YM microorganisms. All specimens were exposed for 211-215 days to a continual flow (2 mL/hr) of 100X J13 simulated water containing 0.1% glucose. These experiments suggest minimal impact of the microbes on the corrosion of Alloy 22 even though the local environment under a biofilm is expected to be different than in the absence of a biofilm. The sterile and microbial anodic polarization curves for both the welded and base metals are very similar. The critical potential, a qualitative indication of breakdown of the passive film, varies between 700 mV for the sterile experiments to 800 mV for the microbial incubated experiments. This difference may be attributed to the biofilm formed on the metal surface. Hysteresis in anodic polarization curves can be a qualitative measure of localized corrosion and is usually characterized by sustaining high current

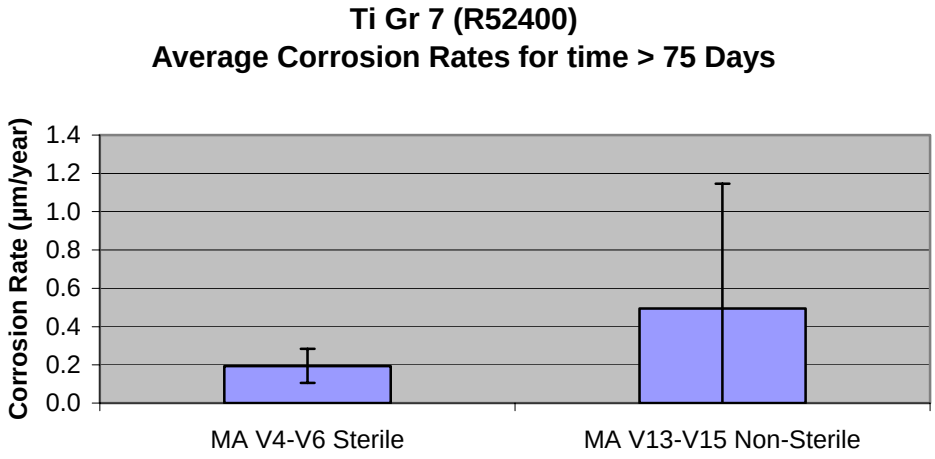

Fig. 10. Average corrosion rates determined by polarization resistance testing of Ti Gr 7 under sterile and non-sterile conditions.

density as the potential is ramped back down, which would represent an inability of the surface to repassivate. The hysteresis observed in both the sterile and microbial inoculated experiments is very narrow in shape, and thus not likely related to the occurrence of localized corrosion. Specimen surfaces were not examined to confirm this conclusion.

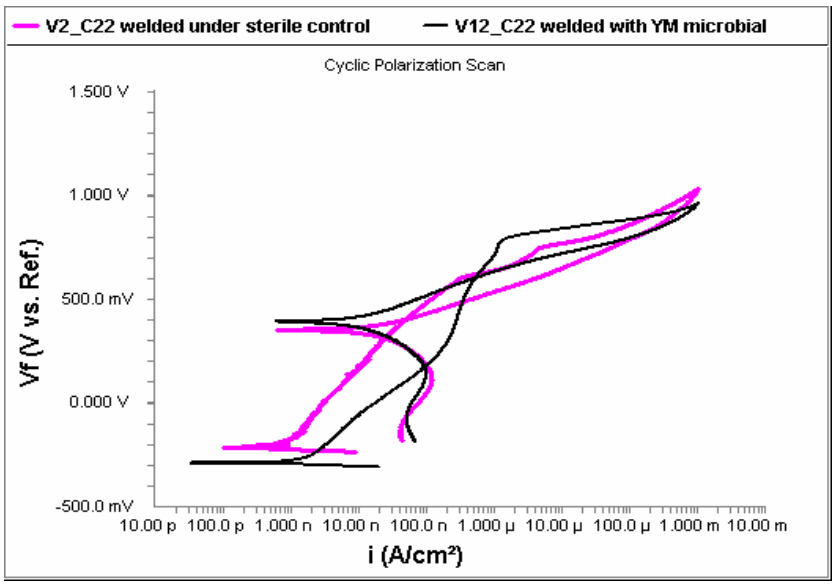

Fig. 11. Comparison of anodic polarization of an Alloy 22 welded metal coupon inoculated and incubated with YM bacteria with a coupon that was incubated under sterile conditions.

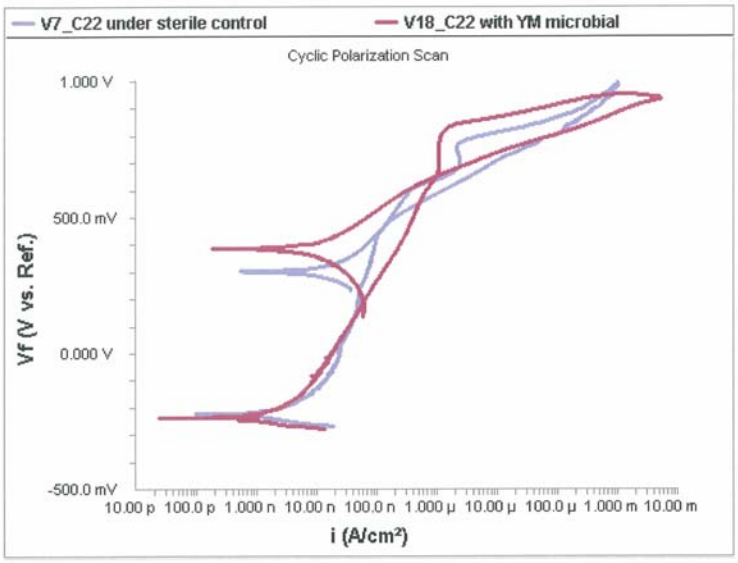

Fig. 12. Comparison of anodic polarization of an Alloy 22 base metal coupon inoculated and incubated with YM bacteria with a coupon that was incubated under sterile conditions.

5.4. Corrosion of Alloy 22 and Composition of the Biofilm

Although the effect of MIC on Alloy 22 is small, both the batch "reduced" experiment and the "oxidizing" flow-through experiment show that inoculated YM bacteria enhance the corrosion of Alloy 22 due to the presence of organic ligands or lower pH within the biofilm. We measured the composition of Alloy 22 films that formed in the sterile and non-sterile systems. Under reducing conditions, soluble Cr (1 ppm) and to a lesser extent Ni (0.1 ppm) were measured when coupons had been incubated with YM microorganisms (13). X-ray photoelectron spectroscopy (XPS) of the biofilm showed a thick carbonaceous layer with both Ni and Cr overlying the biotically incubated coupon (14). In the "oxidizing" system (Fig. 13), the biotically incubated coupon is again covered in a thick carbonaceous biofilm, which is clearly evident even after pre-sputtering for 25 minutes. Within the biofilm, Ni, Cr, and Mo are all evident, as they were in the prior analysis, indicating again the degradation of the alloy under the film, which is nominally at least 4 to 5 times thicker than the passive film formed on Alloy 22 in the sterile system. As the biofilm is traversed, progressing toward the metal surface, the accumulation of alloying elements within the film increased. However, base metal was never reached, as indicated by the lack of asymptotic concentrations of alloying elements. The biofilm also appears to change from an organic-rich film with minimal metal incorporation to a metal-(hydr)oxide-rich film with a smaller contribution from the organic film at depth, as is indicated by a constant oxygen, decreasing carbon, and increasing metal profiles with depth. The increasing hydr(oxide) component at depth reflects the incorporation of dissolved metals by the biofilm. This situation was in contrast to the sterile coupon, which had only a thin carbon surface layer (probably due to glucose in the medium), beneath which the oxidized passive layer is evident by

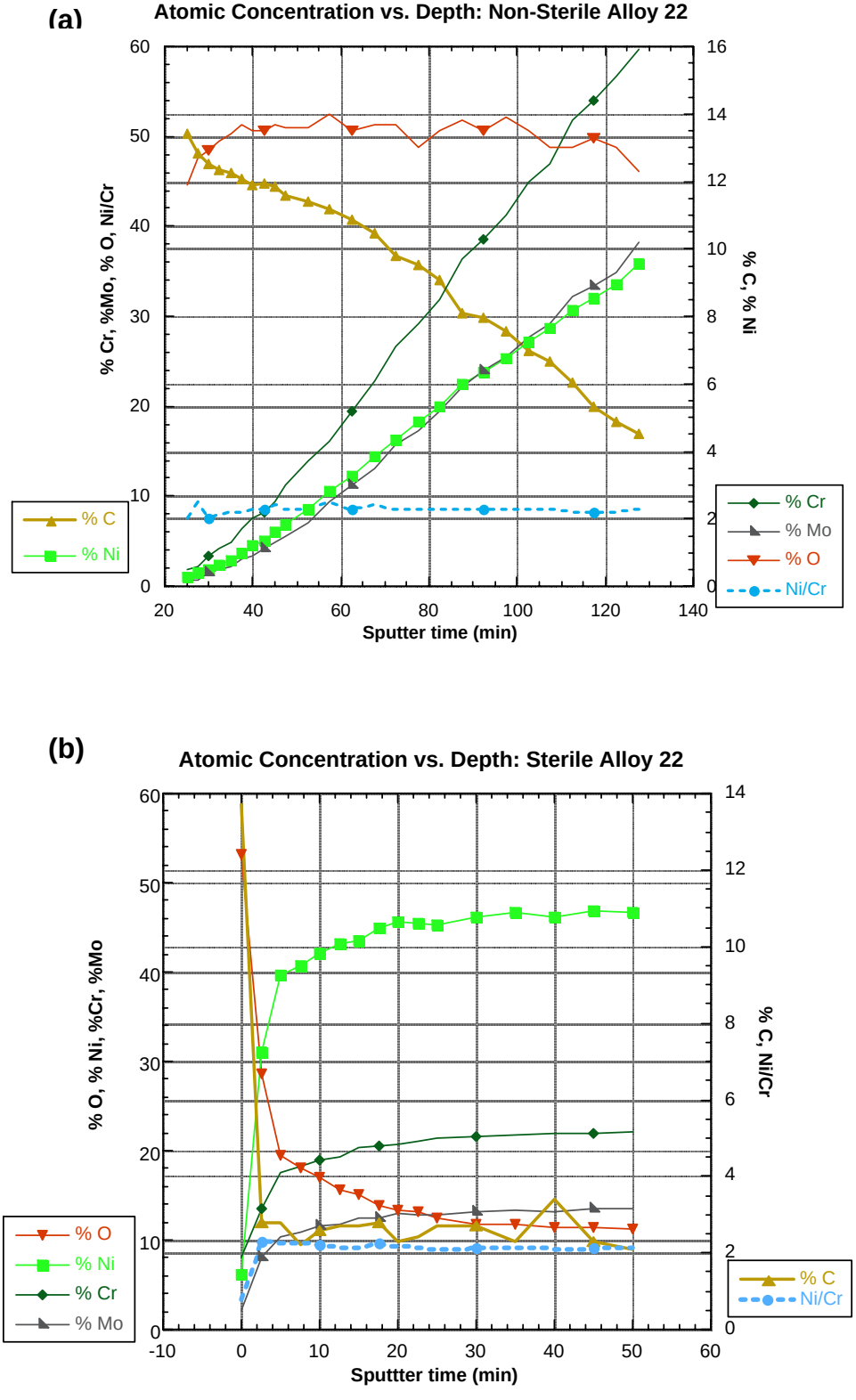

Fig. 13. Relative concentrations (atomic percent) of Alloy 22 alloying elements as a function of depth on: (a) a coupon incubated with YM bacteria and (b) a coupon incubated under sterile conditions.

intermediate levels of oxygen. Then at further depths, all alloying elements reach a steady value, indicating penetration of the base metal.

6. Concluding Remarks

The limiting factor for microbiological growth at Yucca Mountain is the availability of sufficient water either through deliquescence of salts or during groundwater seepage after the thermal pulse. Those microorganisms that do become established during this time, either those able to survive the thermal pulse or those that infiltrate may significantly alter the microbial community that is currently present, as was shown by community analysis of the contents of the LTCTF tanks.

Our experimental results using the present YM community suggest that microbes enhance Alloy 22 corrosion in the presence of a carbon source. Although this effect is small, MIC is seen in the formation of thick biofilm and micropits and in the enhancement of the corrosion rate using electrochemical tests. In addition, it should be noted that the described testing was carried out under relatively mild conditions, at neutral pH, at limited ionic concentrations, and with a carbon source. Further testing under more extreme conditions would need to be conducted to assess those periods during which the repository will experience harsher environmental conditions.

7. References

1. *Engineered Materials Characterization Report for the Yucca Mountain Site Characterization Project*. Vol. 3, Rev. 1, 1997. Section 2.6, Lawrence Livermore National Laboratory, UCRL-ID-119564. Also available as p. 2.6-1 through 2.6-25 of the full report: CRWMS M&O 1997 *Engineered Materials Characterization Report for the Yucca Mountain Site Characterization Project*. Vol. 3, Rev. 1, *Corrosion Data and Modeling*. Las Vegas, Nevada: CRWMS M&O. ACC: MOL.19971009.0589.
2. Horn, J.M., B. Masterson, M. Davis, A. Rivera, A. Miranda, S. Martin. 2004. Bacterial growth dynamics, limiting factors, and community diversity in a subsurface nuclear waste repository environment. *Geomicrobiology J.* **21**, 273–286.
3. Horn, J., C. Carrillo, and V. Dias. 2003. Comparison of the microbial community composition at Yucca Mountain and Laboratory Test Nuclear Repository environments. *Proceedings of Corrosion/2003*, Paper No. 556, National Association of Corrosion Engineers, March 17–20, San Diego, CA.
4. Horn, J., A. Jin, and R. Kelly. 2000. *An Evaluation of Fungal Growth in the Exploratory Studies Facility, Yucca Mountain NV*, Lawrence Livermore National Laboratory, UCRL-ID-141056.
5. *Engineered Materials Characterization Report*. Vol. 3, Rev. 1.1, 1995. Lawrence Livermore National Laboratory, UCRL-ID-119564.
6. Palmer, R.J., J. Siebert, and P. Hirsch. 1991. Biomass and organic acids in sandstone of weathering building: production by bacterial and fungal isolates. *Microb. Ecol.* **21**, 253–266.
7. Schrickx, J.M., M.J.H. Raedts, A.H. Stouthamer, and H.W. van Verseveld. 1995. Organic acid production by *Aspergillus niger* in recycling culture analyzed by capillary electrophoresis. *Anal. Biochem.* **231**, 175–181.
8. Francis, A.J., J.M. Slater, and C.J. Dodge. 1989. Denitrification in deep subsurface sediments. *Geomicrobiology J.* **7**, 103–116.
9. Morris, J.T., G.J. Whiting, and F.H. Chapelle. 1988. Potential denitrification rates in deep sediments from the southeastern coastal plain. *Environ. Sci. Technol.* **22**, 832–836.
10. Martin, S., J. Horn, and C. Carrillo. 2004. Micron-scale MIC of Alloy 22 after long term incubation in saturated nuclear waste repository microcosms. *Proceedings of Corrosion/2004*, Paper No. 04596, National Association of Corrosion Engineers, March 29–April 1, New Orleans, LA.
11. Horn, J., S. Martin, and B. Masterson. 2001. Evidence of biogenic corrosion of titanium after exposure to a continuous culture of *Thiobacillus ferrooxidans* grown in thiosulfate medium. *Proceedings of Corrosion/2001*, Paper No. 259, National Association of Corrosion Engineers, March 12–16, Houston, TX.
12. Lian, T., S. Martin, D. Jones, A. Rivera, and J. Horn. 1999. Corrosion of candidate container materials by Yucca Mountain bacteria. *Proceedings of Corrosion/99*, Paper No. 476, National Association of Corrosion Engineers, May 10–15, San Antonio, TX (Lawrence Livermore National Laboratory, UCRL-JC-132825, January 1999).
13. Horn, J., T. Lian, and S. Martin. 2002. Microbiologically-facilitated effects on the surface composition of Alloy 22, a candidate nuclear waste packaging material. *Proceedings of Corrosion/2002*, Paper No. 02448, National Association of Corrosion Engineers, April 7–11, Denver, CO.
14. BSC (Bechtel SAIC Company) 2004. Appendix 1, Surface Analysis of Corrosion Test Specimens for Dealloying (Response to Container Life and Source Term 1.02), Rev. 1. Las Vegas, Nevada: Bechtel SAIC Company. ACC: MOL.20040923.0130.
15. Cohen, G.N. 2004. *Microbial Biochemistry*. Boston: Kluwer Academic Publishers. 333 p.
16. Nelson, D.L., and Cox, M.M. 2004. *Lehninger Principles of Biochemistry*, Fourth Edition. New York: W.H. Freeman. 1100 p.